ChemComm

COMMUNICATION

View Article Online
View Journal | View Issue



Cite this: *Chem. Commun.*, 2021, **57**, 12464

Received 5th October 2021,
Accepted 26th October 2021

DOI: 10.1039/d1cc05616f

rsc.li/chemcomm

# Macrocyclic complexes based on $[N\cdots I\cdots N]^+$ halogen bonds†

Shilin Yu, [a] Elina Kalenius, [a] Antonio Frontera [b] and Kari Rissanen *[a]

**New 1–2 nm macrocyclic iodine(I) complexes prepared *via* a simple ligand exchange reaction manifest rigid 0.5–1 nm cavities that bind the hexafluorophosphate anion in the gas phase. The size of the cavities and the electrostatic interactions with the iodine(I) cations influence the anion binding properties of these macrocyclic complexes.**

The iodine(I) cation (*aka* iodenium ion) can be considered as an "ultra-polarized" iodine atom that can act as a very strong bis-halogen-bond donor by forming a three-center-four-electron (3c–4e) halogen bond with two Lewis bases (L) resulting in [L–I–L]A (A = anion) complexes[1] with the specific bonding character of the iodine(I) cation.[2] The 3c–4e halogen bond, *viz.* $[N\cdots I\cdots N]^+$, is a robust silver(I)-like building block with enhanced linearity of the N···I···N bond, and thus has great potential as a construction unit for many intricate supramolecular structures. The iconic example of an iodine(I) complex is Barluenga's reagent,[3] bis(pyridine)iodine(I) tetrafluoroborate $[(py)_2I]BF_4$, known in synthetic chemistry as an iodinating agent for aromatic electrophilic substitutions and aromatic amines, yet can also be used as an oxidizing agent.[4–9] However, probably due to the reactivity as an iodinating reagent, the incorporation of iodine(I) as a component in larger supramolecular systems like molecular capsules or cages,[10–13] rotaxanes,[14] monomolecular helicates,[15] and XOFs,[16] has only recently been described. In addition to the "simple" symmetric[1] and asymmetric[17] [L–I–L]A complexes several monomeric clamp-type iodine(I) complexes have been intensely studied by Erdélyi.[18–22] In one case an $I^+$-clamp complex has been suggested to form a dimer, yet it was found to be unstable and experimentally detectable only at low temperatures (−40 °C).[23]

Inspired by the known three ligands (**L1–L3**) and their dimeric silver(I) metallacycles,[24–26] $[(AgL)_2]^{2+}$, and the previously successfully applied[1,10–13,15–17] $[N\cdots Ag\cdots N]^+ \rightarrow [N\cdots I\cdots N]^+$ cation exchange reaction, we envisaged that construction of the corresponding halogen-bonded macrocyclic bis-iodine(I) complexes $[(IL)_2](PF_6)_2$ (**1–3**, Scheme 1) could be achieved. The initial tries with the silver(I) metallacycles and elemental iodine did not proceed cleanly due to the possibility of the metallocycle to open during the exchange reaction and induction of subsequent side reactions, thus an alternative route, *viz.* a ligand exchange reaction previous applied by Dutton[27] for simpler iodine(I) complexes, was successfully used. Using a stable iodine(I) complex bis(1-methyl-1*H*-1,2,3-triazole) iodine(I) hexafluoro-phosphate ($[I(mtz)_2]PF_6$)[28] (see ESI†), and ligands **L1–L3**, the halogen-bonded iodine(I) macrocyclic complexes **1–3** were obtained with 79–87% yield.

The $^1H$ NMR analyses of **1** and **2** (Fig. 1) suggested, as expected, the formation of one highly symmetrical complex. The complexes (**1** or **2**) are kinetically stable and symmetric; the

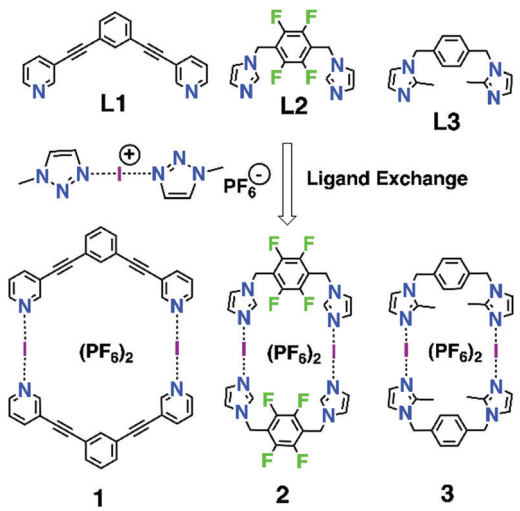


Scheme 1 Ligands **L1–L3** used and the target macrocycles **1–3**.

[a] *University of Jyvaskyla, Department of Chemistry, 40014, Jyväskylä, Finland. E-mail: kari.t.rissanen@jyu.fi*
[b] *Department of Chemistry, Universitat de les Illes Balears, Crts de Valldemossa km 7.6, 07122, Palma de Mallorca Baleares, Spain*

† Electronic supplementary information (ESI) available: Experimental procedures, compounds characterization, DFT calculations. See DOI: 10.1039/d1cc05616f

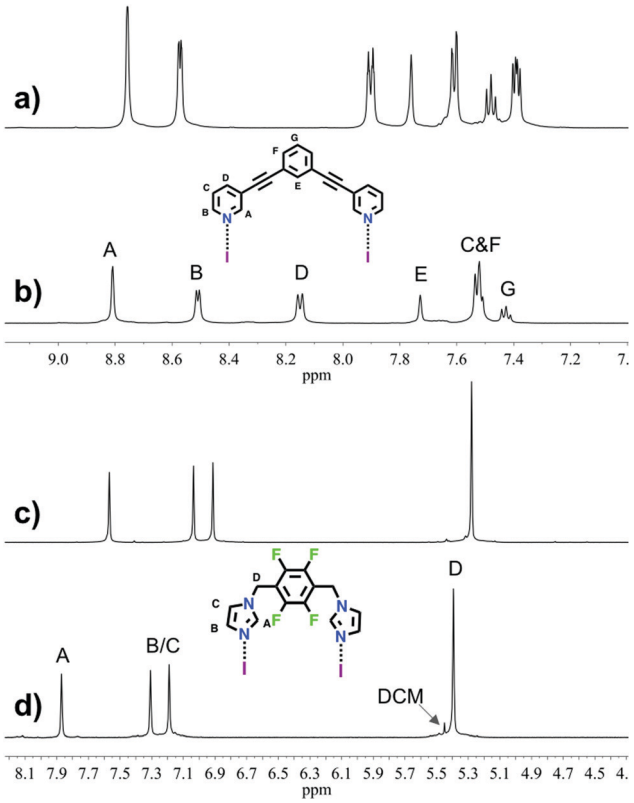


Fig. 1 Selected region of $^1$H NMR spectra (500 MHz, $CD_3CN$, 298 K) for ligand **L1** (a), macrocycle **1** (b), the ligand **L2** (c) and macrocycle **2** (d).

integrals for each of the protons on the ligand remain unchanged, and each peak remains sharp, indicating the formation of only one complex. The downfield shift of the signals ($H_A$, $H_D$ and $H_C$) and the upfield shift of signal $H_B$ for complex **1** as compared to those for **L1** ($\Delta\delta$ = 0.05, 0.25, 0.13 and −0.06 ppm, respectively), and the downfield shift of the signals for complex **2** as compared to those for **L2** ($\Delta\delta$ = 0.30, 0.27, 0.28 and 0.12 ppm, respectively), are characteristic of the iodine–ligand complexation.[17–19,29] The methyl groups in relation with the macrocyclic core result in three district conformations (*up-down-up-down*; *up-up-down-down* and *all-up*) for the methylimidazole complex **3**. The $^1$H NMR spectrum of **3** suggested there are two distinct complexes (Fig. S20, ESI†). The X-ray structures[26,30] of the silver(I) metallacycle from ligand **3** shows only the *up-up-down-down* conformation. Computational studies (see below and ESI†) of the three conformations indicate that the *all-up* is least stable, thus the $^1$H NMR of **3** is interpreted to contain a 60 : 40 ratio of *up-up-down-down* (**3a**) and *up-down-up-down* (**3b**) conformations (see ESI†).

The formation of stable iodine(I) complexes with N···I···N 3c–4e halogen bonds was also confirmed by the N-atom coordination shifts ($\Delta\delta^{15}N_{coord}$) of −90 to −110 ppm (Table 1) in the $^1$H–$^{15}$N HMBC NMR spectra. The two nitrogen atoms are directly involved in the N···I···N 3c–4e bond, which, in combination, results in large chemical shift changes.[31] The values are comparable to the coordination shifts observed in similar iodine(I) complexes (Fig. S25, ESI†).[12,17,18]

Table 1 The $^{15}$N chemical shifts and $^{15}$N coordination shifts for **1–3** ($\Delta\delta^{15}N_{coord} = \delta^{15}N_{complex} - \delta^{15}N_{ligand}$)

| | L1/1 | L2/2 | L3/3a/3b |
|---|---|---|---|
| $\delta^{15}$ | −62.7/−173.3 | −117.3/216.1 | −120.1/−210.1/212.1 |
| $\Delta\delta^{15}N_{coord}$ | −110.6 | −98.8 | −90.5(**3a**)/−92.0(**3b**) |

In order to probe the size of the macrocycles in solution $^1$H DOSY NMR spectra was measured in $CD_3CN$. The diffusion constants for complexes **1–3** are *ca.* two times smaller, evidencing discrete macrocycles two times larger in size than the ligands **L1–L3** (Table S1, ESI†), confirming that these two complexes are dimeric, not monomeric or polymeric.

Despite rigorous attempts X-ray quality crystals of **1–3** were not obtained. Large basis set DFT calculations have been applied for the macrocycles **1–3** (Fig. 3 and Fig. S32, ESI†). The geometries of the optimized complexes have been compared with the X-ray structures of the corresponding silver(I) metallacycles retrieved from the CSD database. In general, the optimized geometries of the macrocyclic XB complexes (**1–3**) are very similar to the X-ray geometries of the corresponding silver(I) metallacycles.

The main structural difference is that the N···I···N angles in **1–3** are more linear than the N···Ag···N analogues. Moreover, the intra-complex $I^+\cdots I^+$ distances are shorter than the $Ag^+\cdots Ag^+$ distances in complexes **1** and **2** and longer in complex **3** (see Fig. 2), their variations are very likely caused by the different packing and anion–cation interactions in the solid-state of the silver(I) metallacycles.

The stoichiometries and structures of the complexes were further verified using electrospray ionization ion mobility mass spectrometry (ESI-IMMS). In gas phase, the complexes were observed to complex the $PF_6^-$ anion into the cavity of the macrocycle and ions $[\mathbf{1}\text{-}PF_6]^+$, $[\mathbf{2}\text{-}PF_6]^+$ and $[\mathbf{3}\text{-}PF_6]^+$ appeared in spectra with high abundance (ESI,† Fig. S28–S30 and Fig. 3.) The MS/MS analysis also confirmed the composition as $[2L + 2I + PF_6]^+$ and showed structure-related dissociation of macrocycles through consecutive eliminations of $IPF_6$ or $HPF_6$ and ligands **L1**, **L2** or **L3**.

The correlation between theoretical and experimental structures was further analyzed by ion-mobility mass spectrometry experiments.[32] To visualize the IM-MS data, $[\mathbf{1,2,3}\text{-}PF6]^+$ complexes were DFT-optimized (Fig. 4). The calculations show that the cavity in **2** or **3** just suitable for the $PF_6^-$ anion which fits very well inside the cavity, as evidenced by the optimized geometries of the host–guest complexes. An interesting combination of non-covalent interactions is formed. The complex $[\mathbf{2}\text{-}PF_6]^+$ manifests two anion–π interactions, due to the presence of two electron-deficient tetrafluorophenyl rings in the macrocycle (marked as red dashed lines in Fig. 4a). In fact, two fluorine atoms of the anion point to the center of the electron-deficient rings (distance 3.16 Å). Additional $C_{sp}2$–H···F HBs (2.37 Å) and electrostatic forces $I^+\cdots PF_6^-$ firmly hold the guest inside the cavity. The orientation of the anionic guest is different in $[\mathbf{3}\text{-}PF_6]^+$ because the aromatic rings of the macrocycle are electron-rich. In this case the four fluorine

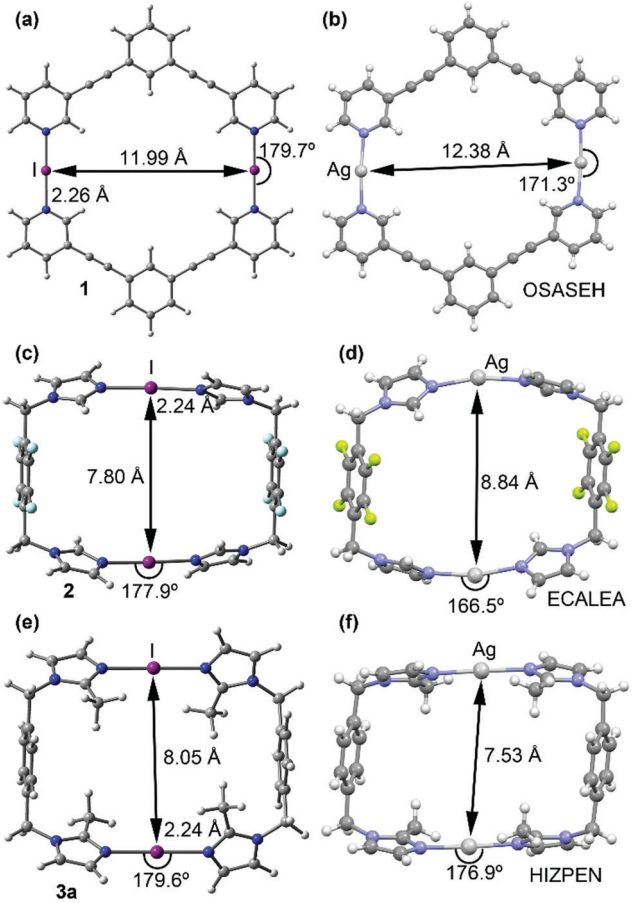


Fig. 2 Optimized geometries of compounds **1** (a), **2** (b) and **3a** (c) at the M06-2X/def2TZVp level of theory. The X-ray structures of the corresponding Ag(I) metallacycles (CSD refcodes OSASEH (b) and ECALEA (d) and HIZPEN (f)).

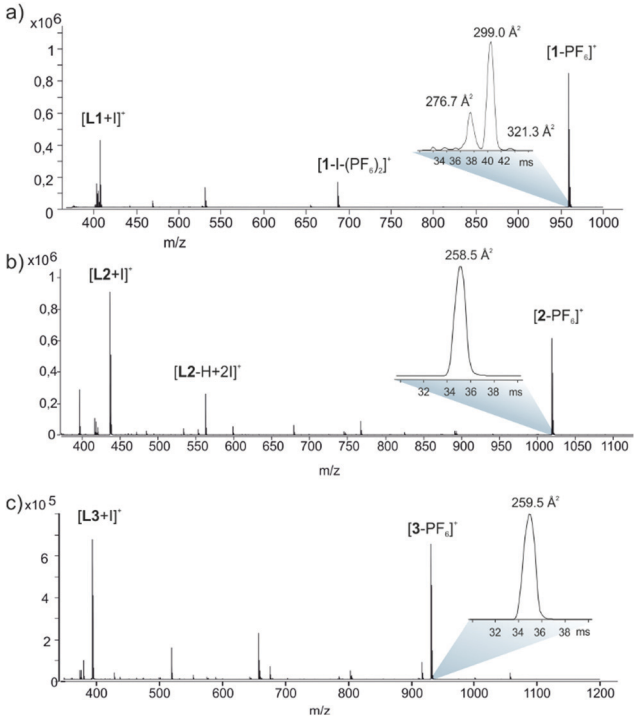


Fig. 3 (+)ESI-QTOF mass spectrum (a) **1**, (b) **2** and (c) **3** in MeCN. Insets show IM-TOF arrival time distributions for ions [**C**-PF6]$^+$.

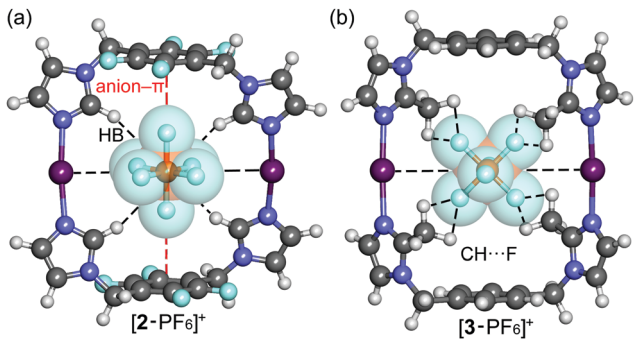


Fig. 4 Optimized structures of host–guest complexes of macrocycles **2** (a) and **3** (b) with the $PF_6^-$ anion at the M06-2X/def2-TZVP level of theory.

atoms of the anion point towards the methyl groups, establishing multiple $C_{sp^3}$–H···F contacts (distances 2.48–2.54 Å). The [**3**-$PF_6$]$^+$ host–guest complex is further stabilized by $I^+\cdots PF_6^-$ ion pair interactions. The IM-MS arrival time distributions (ATDs) showed single drift peaks for the host–guest complexes [**2**-$PF_6$]$^+$ and [**3**-$PF_6$]$^+$. The experimentally observed collision cross section values using He as a drift gas ($^{DT}CCS_{He}$) for these ions were 184.4 Å$^2$ and 182.3 Å$^2$, respectively. The values show nice correlation (<1.9% difference) with theoretical CCS values ($^{TMLJ}CCS_{He}$) calculated on basis of DFT-optimized structures (Table S3, ESI†). This comparison between theoretical and experimental results verifies macrocyclic structure, analogues to $Ag^+$ complexes, also in the gas phase. This further suggests that the $PF_6$ anion act as a guest and is located inside the macrocycle. The two conformers observed in $^1$H NMR spectra for **3** could not be resolved by IM-MS, because the theoretical $^{TMLJ}CCS_{He}$ values for **3a** and **3b** differ only by 0.98 Å$^2$ (typically ~1% difference is expected to be resolved with ultra-high resolving power instruments).[32] The IM drift peak for [**3**-$PF_6$]$^+$ has, however, clearly decreased resolution ($R_{FWHM}$ for [**3**-$PF_6$]$^+$ is only 29.7 whereas for [**2**-$PF_6$]$^+$ $R_{FWHM}$ = 46.3), which often indicates several closely related, unresolved conformers.

The ATD for much larger [**1**-$PF_6$]$^+$ surprisingly shows distribution of IM drift peaks ranging from 196.6 to 237.8 Å$^2$. The DFT optimization confirm, that the cavity in **1** is much larger than the size of $PF_6$ anion, allowing different locations for a guest within the cavity (see Fig. S32a (ESI†) for one possible host–guest complex). To study this, the structures of *endo* and *exo* complexes for [**1**-$PF_6$]$^+$ were calculated, resulting in $^{TMLJ}CCS_{He}$ values of 228.8 and 231.8 Å$^2$, respectively. Whereas in [**2**-$PF_6$]$^+$ and [**3**-$PF_6$]$^+$ the anion has a tight fit, the complexation of $PF_6^-$ into the larger cavity of [**1**-PF6]$^+$ results in less specific interactions with the cavity walls and offers larger degrees of freedom for the spatial location of the guest. We conclude that the multiple IM peaks originate from the different locations of loosely bound $PF_6^-$ counter anion.

 

Also according to the MS measurements the $[\mathbf{1}\text{-}PF_6]^+$ complex is less stable (has lower interaction energy), which is reflected in MS/MS spectra (collision induced dissociation, CID) showing more dissociation and lower relative intensity for $[\mathbf{1}\text{-}PF_6]^+$ precursor ion when compared with the $[\mathbf{2}\text{-}PF6]^+$ and $[\mathbf{3}\text{-}PF6]^+$ precursor ions.

In summary, we have demonstrated a simple preparation of three new iodine(I)-based macrocycles *via* ligand exchange reaction, and studied their structures and host–guest behavior using $^1H$ and $^1H$–$^{15}N$ HMBC and DOSY NMR, IM-MS and theoretical calculations. Further studies of these systems are underway in our laboratory. The simple preparation route to the previously unreported iodine(I) macrocycles might provide a way to construct iodine(I)-based mechanically interlocked molecules.

We gratefully acknowledge financial support from the Academy of Finland (K. R. grant no. 317259), the MICIU/AEI of Spain (A. F. project CTQ2017-85821-R FEDER), and the University of Jyvaskyla, Finland.

## Conflicts of interest

There are no conflicts to declare.

## Notes and references

1 L. Turunen and M. Erdélyi, *Chem. Soc. Rev.*, 2020, **49**, 2688–2700.
2 L. Turunen and M. Erdélyi, in *Halogen Bonding in Solution*, ed. S. Huber, Wiley-VCH Verlag GmbH, 2021, pp. 121–151.
3 J. Barluenga, F. González-Bobes, M. C. Murguía, S. R. Ananthoju and J. M. González, *Chem. – Eur. J.*, 2004, **10**, 4206–4213.
4 J. A. Creighton, I. Haque and J. L. Wood, *Chem. Commun.*, 1966, 229.
5 J. A. Creighton, I. Haque and J. L. Wood, *Chem. Commun.*, 1966, 892.
6 I. Haque and J. L. Wood, *J. Mol. Struct.*, 1968, **2**, 217–238.
7 J. Barluenga, J. M. González, M. A. Garcia-Martin, P. J. Campos and G. Asensio, *J. Chem. Soc., Chem. Commun.*, 1992, 1016–1017.
8 J. Ezquerra, C. Pedregal, C. Lamas, J. Barluenga, M. Pérez, M. A. García-Martín and J. M. González, *J. Org. Chem.*, 1996, **61**, 5804–5812.
9 G. Espuña, G. Arsequell, G. Valencia, J. Barluenga, M. Pérez and J. M. González, *Chem. Commun.*, 2000, 1307–1308.
10 L. Turunen, U. Warzok, C. A. Schalley and K. Rissanen, *Chem*, 2017, **3**, 861–869.
11 U. Warzok, M. Marianski, W. Hoffmann, L. Turunen, K. Rissanen, K. Pagel and C. A. Schalley, *Chem. Sci.*, 2018, **9**, 8343–8351.
12 L. Turunen, A. Peuronen, S. Forsblom, E. Kalenius, M. Lahtinen and K. Rissanen, *Chem. – Eur. J.*, 2017, **23**, 11714–11718.
13 L. Turunen, U. Warzok, R. Puttreddy, N. K. Beyeh, C. A. Schalley and K. Rissanen, *Angew. Chem., Int. Ed.*, 2016, **55**, 14033–14036.
14 M. Kandrnálová, Z. Kokan, V. Havel, M. Nečas and V. Šindelář, *Angew. Chem., Int. Ed.*, 2019, **58**, 18182–18185.
15 A. Vanderkooy, A. K. Gupta, T. Földes, S. Lindblad, A. Orthaber, I. Pápai and M. Erdélyi, *Angew. Chem., Int. Ed.*, 2019, **58**, 9012–9016.
16 G. Gong, S. Lv, J. Han, F. Xie, Q. Li, N. Xia, W. Zeng, Y. Chen, L. Wang, J. Wang and S. Chen, *Angew. Chem., Int. Ed.*, 2021, **60**, 14831–14835.
17 J. S. Ward, G. Fiorini, A. Frontera and K. Rissanen, *Chem. Commun.*, 2020, **56**, 8428–8431.
18 A.-C. C. Carlsson, K. Mehmeti, M. Uhrbom, A. Karim, M. Bedin, R. Puttreddy, R. Kleinmaier, A. A. Neverov, B. Nekoueishahraki, J. Gräfenstein, K. Rissanen and M. Erdélyi, *J. Am. Chem. Soc.*, 2016, **138**, 9853–9863.
19 A.-C. C. Carlsson, J. Gräfenstein, A. Budnjo, J. L. Laurila, J. Bergquist, A. Karim, R. Kleinmaier, U. Brath and M. Erdélyi, *J. Am. Chem. Soc.*, 2012, **134**, 5706–5715.
20 A. A. Neverov, H. X. Feng, K. Hamilton and R. S. Brown, *J. Org. Chem.*, 2003, **68**, 3802–3810.
21 L. Turunen, F. B. Németh, D. A. Decato, I. Pápai, O. B. Berryman and M. Erdélyi, *Bull. Chem. Soc. Jpn.*, 2020, **94**, 191–196.
22 S. Lindblad, F. Boróka Németh, T. Földes, D. von der Heiden, H. G. Vang, Z. L. Driscoll, E. R. Gonnering, I. Pápai, N. Bowling and M. Erdélyi, *Chem. – Eur. J.*, 2021, **27**, 13748–13756.
23 S. Lindblad, K. Mehmeti, A. X. Veiga, B. Nekoueishahraki, J. Gräfenstein and M. Erdélyi, *J. Am. Chem. Soc.*, 2018, **140**, 13503–13513.
24 K. J. Kilpin, M. L. Gower, S. G. Telfer, G. B. Jameson and J. D. Crowley, *Inorg. Chem.*, 2011, **50**, 1123–1134.
25 Y. Gao, B. Twamley and J. M. Shreeve, *Inorg. Chem.*, 2006, **45**, 1150–1155.
26 L. Dobrzańska, G. O. Lloyd, H. G. Raubenheimer and L. J. Barbour, *J. Am. Chem. Soc.*, 2005, **127**, 13134–13135.
27 D. C. Georgiou, P. Butler, E. C. Browne, D. J. D. Wilson and J. L. Dutton, *Aust. J. Chem.*, 2013, **66**, 1179–1188.
28 S. Yu, P. Kumar, J. S. Ward, A. Frontera and K. Rissanen, *Chem*, 2021, **7**, 948–958.
29 M. Bedin, A. Karim, M. Reitti, A.-C. C. Carlsson, F. Topić, M. Cetina, F. Pan, V. Havel, F. Al-Ameri, V. Sindelar, K. Rissanen, J. Gräfenstein and M. Erdélyi, *Chem. Sci.*, 2015, **6**, 3746–3756.
30 M. du Plessis, V. J. Smith and L. J. Barbour, *CrystEngComm*, 2014, **16**, 4126–4132.
31 S. B. Hakkert, J. Gräfenstein and M. Erdélyi, *Faraday Discuss.*, 2017, **203**, 333–346.
32 A. T. Kirk, A. Bohnhorst, C.-R. Raddatz, M. Allers and S. Zimmermann, *Anal. Bioanal. Chem.*, 2019, **411**, 6229–6246.